

## Supporting Information

### High-Performance BaZr<sub>0.35</sub>Ti<sub>0.65</sub>O<sub>3</sub> Thin Film Capacitors with Ultrahigh Energy Storage Density and Excellent Thermal Stability

Zhongshuai Liang,<sup>a,b</sup> Ming Liu\*,<sup>a,b</sup> Chunrui Ma,<sup>b</sup> Lvkang Shen,<sup>a,b</sup> Lu Lu,<sup>a,b</sup> and Chun-Lin Jia<sup>a,b,c</sup>

---

<sup>a</sup> School of Microelectronics, Xi'an Jiaotong University, Xi'an 710049, China

<sup>b</sup> State Key Laboratory for Mechanical Behavior of Materials, Xi'an Jiaotong University, Xi'an 710049, P. R. China.

<sup>c</sup> Ernst Ruska Centre for Microscopy and Spectroscopy with Electrons, Forschungszentrum Jülich, D-52425 Jülich, Germany

\* E-mail: m.liu@xjtu.edu.cn

Electronic Supplementary Information (ESI) available: [details of any supplementary information available should be included here]. See DOI: 10.1039/x0xx00000x

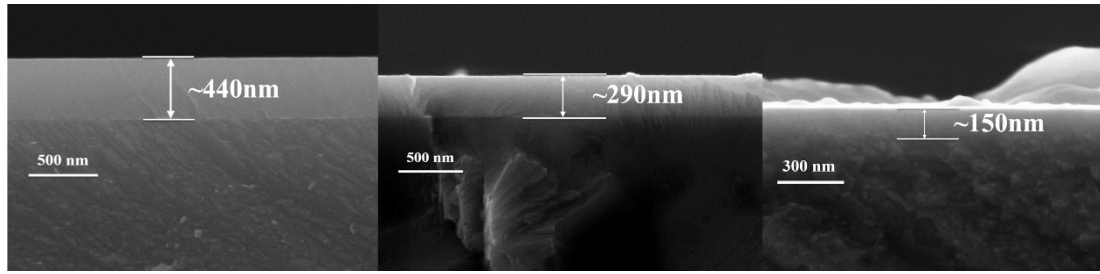


Fig. S1 The cross-sectional scanning electron microscope images of BZT/Nb:SrTiO<sub>3</sub> heterostructure.

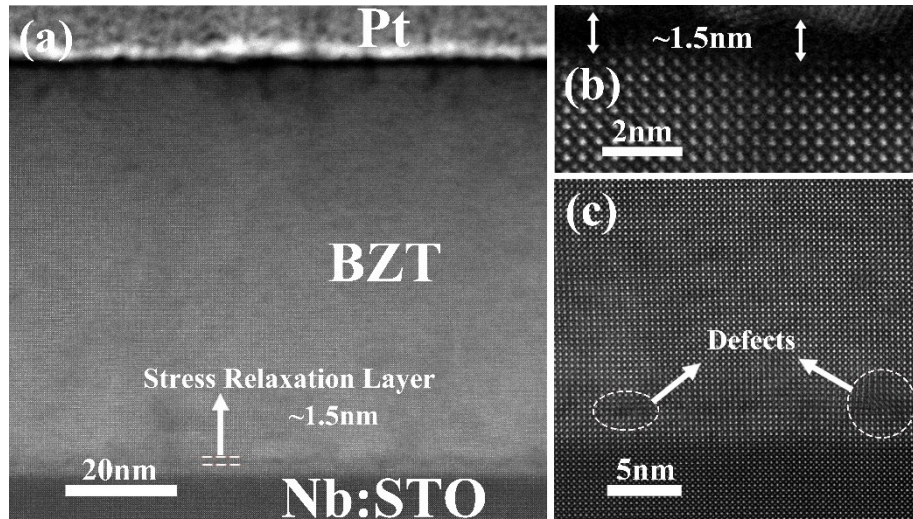


Fig. S2 Cross-sectional HAADF TEM images of (a) the Pt/BZT/NSTO; (b) the Pt/BZT interface; (c) the BZT/NSTO interface. The arrows in the Fig. S2b mark the interfacial layer at the interface of the BZT.

The interfacial layer ( $\sim 1.5\text{nm}$ ) between the BZT films and the Pt electrodes were generated by the high-energy platinum ion impact damage, since the Pt electrodes were fabricated with highly energetic growth processes (DC sputtering), as shown in the Fig. S2b. Besides, from the Fig. S2a, there exists a stress relaxation layer ( $\sim 1.5\text{nm}$ ) in the BZT films. And the enriched defects were found in the relaxation layer, as shown in the Fig. S2c. Therefore, the total thickness of the interfacial layer was about 3nm.

We have estimated the dielectric constant of the bulk films and the interfacial layer

by fitting the ' $d/\varepsilon - d$ ' curves, as shown in the Fig. S3 and Table S1. The  $d$  and  $\varepsilon$  are the thickness and the dielectric constant at 1 kHz of the BZT films respectively. The calculation formula was show below:

$$\frac{d}{\varepsilon} = \frac{d_b}{\varepsilon_b} + \frac{d_i}{\varepsilon_i} = \frac{d - d_i}{\varepsilon_b} + \frac{d_i}{\varepsilon_i} = \frac{d}{\varepsilon_b} + d_i \left( \frac{1}{\varepsilon_i} - \frac{1}{\varepsilon_b} \right)$$

where the  $d_e$ ,  $\varepsilon_e$ ,  $d_i$  and  $\varepsilon_i$  are the bulk dielectric film thickness, the dielectric constant of the bulk dielectric film, the interfacial layer thickness and the dielectric constant of the interfacial layer of the BZT films, respectively.<sup>1</sup>

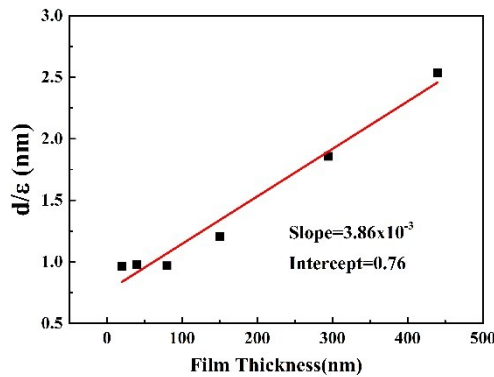


Fig. S3 The  $d/\varepsilon$  at 1 kHz as a function of the BZT thickness from the 20nm to 440nm.

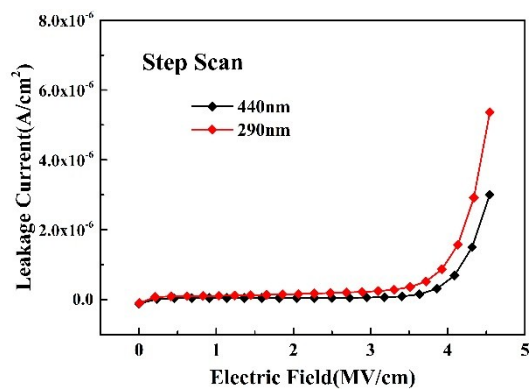


Fig. S4 Current-voltage characteristics of the 440nm-thick and 290nm-thick BZT films in this work.

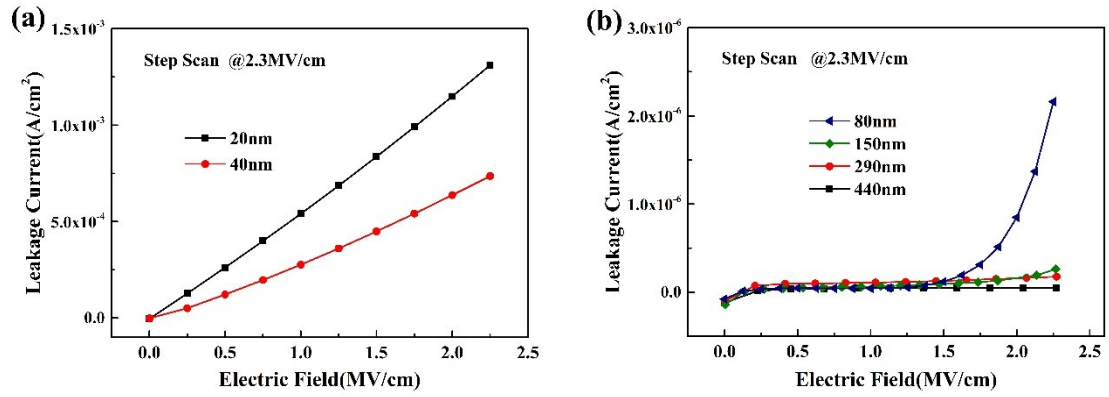


Fig. S5 Current-voltage characteristics of (a) the 20nm-thick and 40nm-thick BZT films in this work, (b) the 80nm-thick to 440nm-thick BZT films in this work.

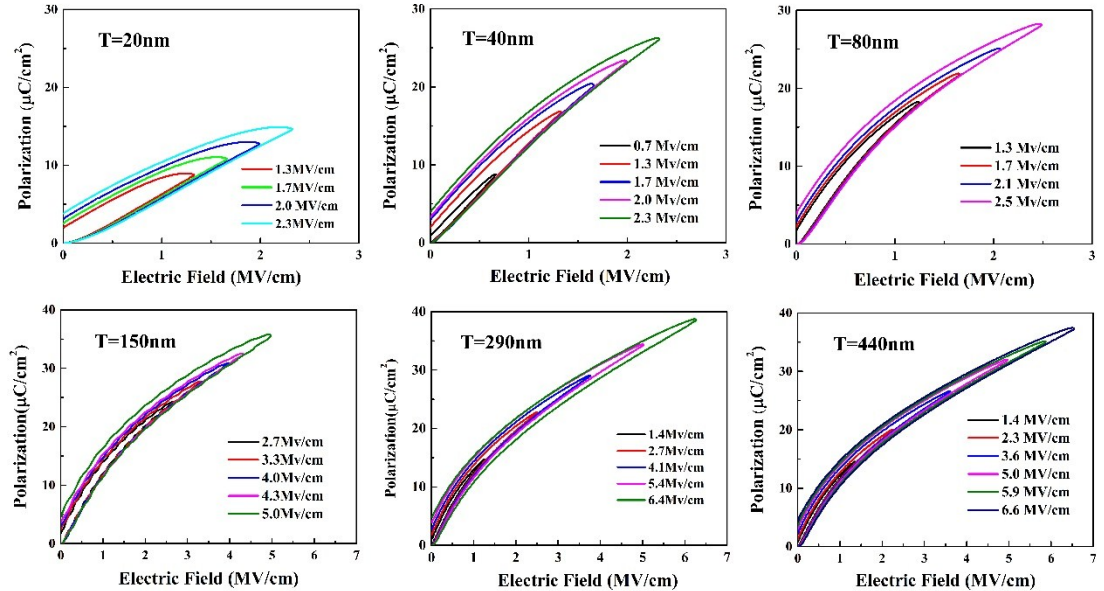


Fig. S6 The unipolar P-E loops under different electric field at 1 kHz at room temperature of various thickness BZT film capacitors from 20nm to 40nm.

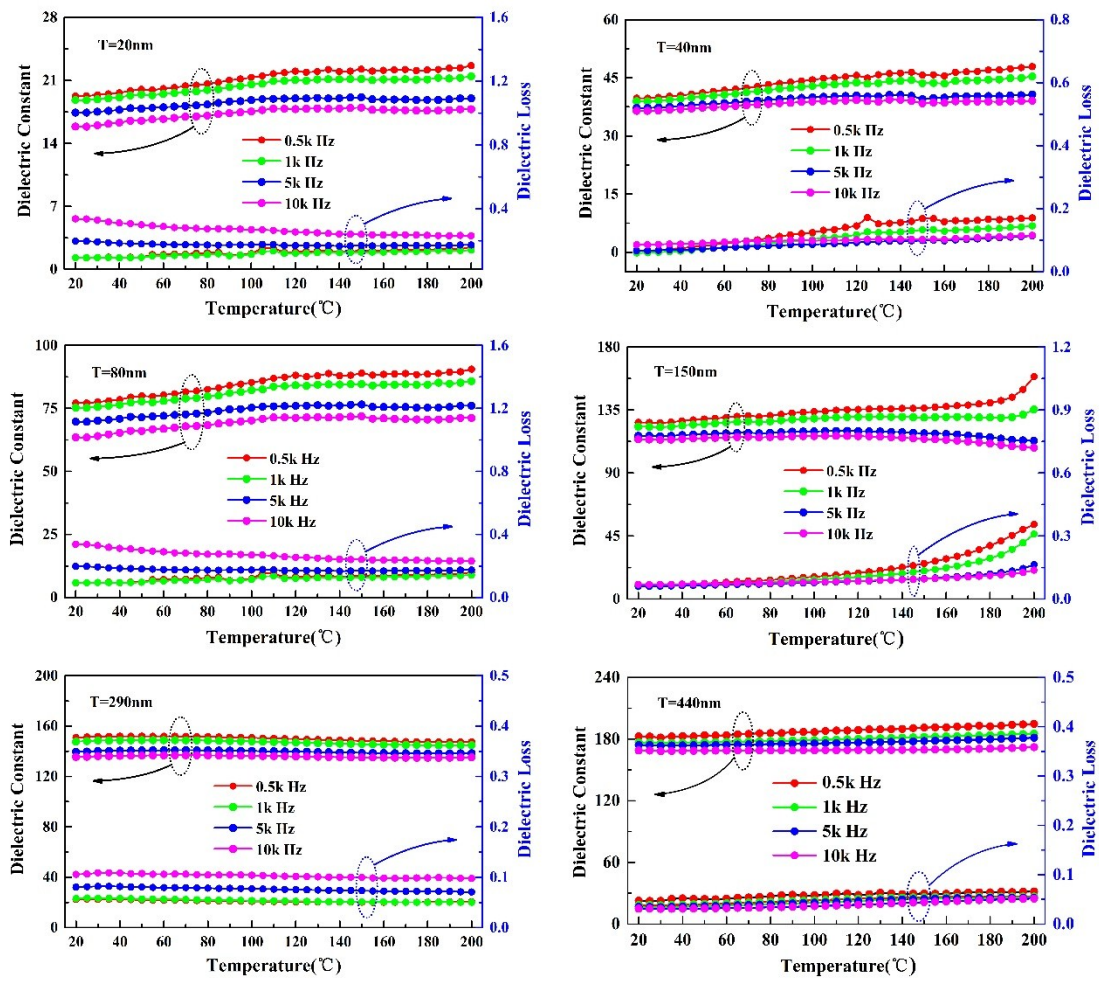


Fig. S7 Temperature dependence of dielectric permittivity and dielectric loss at various frequencies for BZT film capacitors with thicknesses in range from 20nm to 40nm.

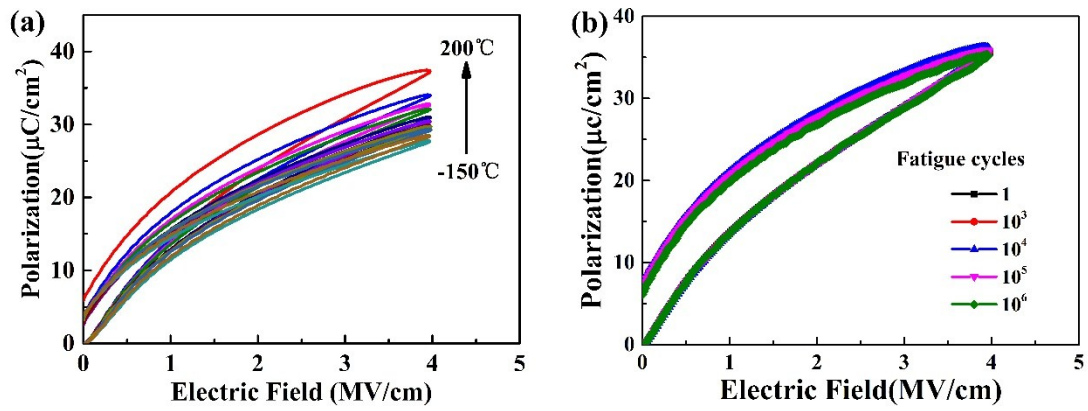


Fig. S8 The unipolar P-E loops measured under 4.0MV/cm at 1 kHz (a) at different temperature of the 440nm-thick BZT film capacitors; (b) at 200 °C with different fatigue cycles state of the 440nm-thick BZT film capacitors.

Table S1 The calculation results of the bulk dielectric film dielectric constant ( $\varepsilon_b$ ) and the dielectric constant of the interfacial layer ( $\varepsilon_i$ ).

$\varepsilon_b$	$\frac{d_i}{\varepsilon_i}$	$\varepsilon_i$
259.1	0.76	4.0

Table S2 Comparison of the energy storage density ( $W_{rec}$ ) and energy efficiency ( $\eta$ ) at room temperature among the 440-nm-thick BZT film capacitors and other representative promising ceramic

	Materials	$W_{rec}$ (J/cm <sup>3</sup> )	$\eta$
<b>This work</b>	<b>BZT/NSTO</b>	<b>78.7</b>	<b>80.5%</b>
Pb-Free	Bi <sub>1.5</sub> Zn <sub>0.9</sub> Nb <sub>1.35</sub> Ta <sub>0.15</sub> O <sub>6.9</sub> <sup>[2]</sup>	40.2	80%
	0.4BiFeO <sub>3</sub> -0.6SrTiO <sub>3</sub> <sup>[3]</sup>	18.6	85%
	Hf <sub>0.3</sub> Zr <sub>0.7</sub> O <sub>2</sub> <sup>[4]</sup>	46	—
	0.88BaTiO <sub>3</sub> -0.12Bi(Mg, Ti)O <sub>3</sub> <sup>[5]</sup>	37	—
Pb-Based	Pb <sub>0.92</sub> La <sub>0.08</sub> Zr <sub>0.52</sub> Ti <sub>0.48</sub> O <sub>3</sub> <sup>[6]</sup>	85	—
	Pb <sub>0.96</sub> La <sub>0.04</sub> Zr <sub>0.98</sub> Ti <sub>0.02</sub> O <sub>3</sub> <sup>[7]</sup>	61	33%
	Bi(Ni <sub>1/2</sub> Ti <sub>1/2</sub> )O <sub>3</sub> -PbTiO <sub>3</sub> <sup>[8]</sup>	45.1	43.4%
	Pb <sub>0.85</sub> Ba <sub>0.05</sub> La <sub>0.10</sub> Zr <sub>0.90</sub> Ti <sub>0.10</sub> O <sub>3</sub> <sup>[9]</sup>	42.3	68%
	Pb <sub>0.8</sub> Ba <sub>0.2</sub> ZrO <sub>3</sub> <sup>[10]</sup>	40.2	64.1%
	Pb <sub>0.97</sub> Y <sub>0.02</sub> [(Zr <sub>0.6</sub> Sn <sub>0.4</sub> ) <sub>0.925</sub> Ti <sub>0.075</sub> ]O <sub>3</sub> <sup>[11]</sup>	21	91.9%

dielectric oxide film capacitors reported previously.

## **References:**

1. L. J. Sinnamon, R. M. Bowman, and J. M. Gregg, *Appl. Phys. Lett.*, 2001, **78**, 1724-1726.
2. E. K. Michael and S. Troliermckinstry, *J. Appl. Phys.*, 2015, **118**, 234102.
3. T. M. Correia, M. McMillen, M. K. Rokosz, P. M. Weaver, J. M. Gregg, G. Viola and M. G. Cain, *J. Am. Ceram. Soc.*, 2013, **96**, 2699–2702.
4. M. H. Park, H. J. Kim, Y. J. Kim, T. Moon, K. D. Kim and C. S. Hwang, *Adv. Energy Mater.* 2014, **4**, 1400610.
5. P. C. Joshi and S. B. Desu, *J. Appl. Phys.*, **80**, 2349-2357.
6. U. Balachandran, M. Narayanan, S. Liu and B. Ma, *Jpn. J. Appl. Phys.*, 2013, **52**, 05DA10.
7. Z. Hu, B. Ma, R. E. Koritala and U. Balachandranl, *Appl. Phys. Lett.*, 2014, **104**, 263902.
8. Z. Xie, B. Peng, S. Meng, Y. Zhou and Z. Yue, *J. Am. Ceram. Soc.*, 2013, **96**, 2061–2064.
9. H. C. Gao, N. N. Sun, Y. Li, Q. W. Zhang, X. H. Hao, L. B. Kong, Q. Wang, *Ceram. Int.*, 2016, **42** 16439–16447.
10. B. Peng, Q. Zhang, X. Li, T. Sun, H. Fan, S. Ke, M. Ye, Y. Wang, W. Lu, H. Niu, X. Zeng and H. Huang, *ACS Appl. Mater. Interfaces*, 2015, **7**, 13512–13517.
11. C. W. Ahn, G. Amarsanaa, S. S. Won, S. A. Chae, D. S. Lee and I. W. Kim, *ACS Appl. Mater. Interfaces*, 2015, **7**, 26381–26386.